

# Seasonal fluctuations in the advance of a tidewater glacier and potential causes: Hubbard Glacier, Alaska, USA

J. Brent RITCHIE, Craig S. LINGLE, Roman J. MOTYKA, Martin TRUFFER

*Geophysical Institute, University of Alaska Fairbanks, 903 Koyukuk Drive, Fairbanks, Alaska 99775-7320, USA  
E-mail: brent.ritchie@gi.alaska.edu*

**ABSTRACT.** Satellite imagery has been used to acquire seasonal terminus positions of tidewater Hubbard Glacier, Alaska, USA, from 1992 to 2006. During this 15 year time period, the width-averaged advance of the entire terminus has been  $\sim 620$  m at a mean rate of  $35 \text{ m a}^{-1}$ . Seasonal fluctuation of the terminus ranges from 150 to 200 m on average and varies spatially. A section of the terminus, near a narrow gap where the glacier has now twice closed off 40 km long Russell Fiord, exhibited little to no mean advance during this time period but displayed seasonal fluctuations of 300–500 m. Seasonal variability in surface ice speeds and surface sea-water temperatures was also observed; both are potential forcing mechanisms for terminus fluctuations. Seasonal changes in sea-water temperature of  $10\text{--}12^\circ\text{C}$ , as well as seasonal changes in subglacial freshwater discharge, are inferred to influence calving and submarine melting at the terminus, driving seasonal variations. Displacements of the medial moraine separating Hubbard and Valerie Glaciers at the terminus suggest surge-like pulses of the latter, with a periodicity of several years. The timing of these pulses suggests they may influence the Hubbard terminus near Gilbert Point and have implications for future closures of Russell Fiord.

## 1. INTRODUCTION

The unique, dynamic behavior of tidewater glaciers is strongly influenced by calving of ice at the terminus. The rate of advance or retreat of the terminus is

$$\frac{dL}{dt} = \bar{v}_s - \bar{v}_c, \quad (1)$$

where  $L$  is the length of the glacier,  $\bar{v}_s$  is the width-averaged ice speed at the terminus and  $\bar{v}_c$  is the width-averaged calving speed at the terminus. In terms of water equivalent volume fluxes, Equation (1) can be expressed

$$Q_t = Q_{in} - Q_c, \quad (2)$$

where  $Q_t$  is the rate at which ice volume is added or lost at the terminus,  $Q_{in}$  is the ice flux into the terminus and  $Q_c$  is the calving flux (including ice loss caused by both iceberg calving and submarine melting) (O'Neel and others, 2003). Many studies have been conducted in order to understand the dynamics of tidewater glaciers (e.g. Meier and Post, 1987; O'Neel and others, 2001; Pfeffer, 2007), and particularly tidewater calving (e.g. Brown and others, 1982; Van der Veen, 2002; Motyka and others, 2003; Benn and others, 2007, and references therein). Debate continues however, regarding the factors influencing calving and tidewater glacier dynamics. Calving can remove large amounts of ice from glaciers and ice sheets in relatively short times, particularly during catastrophic retreats. For example, Krimmel (2001) documented calving rates as high as  $20 \times 10^6 \text{ m}^3 \text{ d}^{-1}$  at Columbia Glacier, Alaska, USA. The rapid disintegration of the Northern Hemisphere Pleistocene ice sheets appears to have partly taken place by calving into proglacial lakes as well as by rapid calving retreat of ice streams grounded below sea level (e.g. Van der Veen, 1999, and references therein). A significant portion of mass loss from both the Greenland ice sheet (about 56%; Reeh, 1994) and the Antarctic ice sheet (about 77%; Jacobs and others, 1992) is due to calving from outlet glaciers having both floating and grounded termini. The recently reported rapid

changes in Greenland are also due in large part to increased calving (e.g. Rignot and Kanagaratnam, 2006).

Previous studies of grounded tidewater glaciers have shown that annually averaged calving rates are correlated with water depth at the calving front (Brown and others, 1982; Pelto and Warren, 1991). Additional studies have shown that this correlation does not hold on a seasonal or shorter timescale (Sikonia, 1982; Van der Veen, 1996; Motyka and others, 2003). Sikonia (1982) argued for a correlation between water discharge at the bed and seasonal calving rates. All these relationships are empirical. A study of LeConte Glacier, southeast Alaska, by Motyka and others (2003) showed that submarine melting can be an important seasonal contribution to ice loss at the face of tidewater glaciers. The controlling factor is forced convection at the ice–water interface driven by subglacial discharge of fresh water and the influx of warm saline water. Van der Veen (2002) suggested that the terminus position is maintained by the height of the ice face above flotation. In this model, the calving rate is determined by both glacier speed and thickness change at the terminus. Given these ideas, the factors influencing calving rate appear to be a complex combination of many factors. Given that  $dL/dt$  is between one and two orders of magnitude smaller than either the ice velocity or the calving rate, it seems clear that these two cannot be entirely independent of each other (Equation (1)).

Tidewater glaciers have been shown to exhibit seasonal variations in their terminus positions (Meier and Post, 1987; Sohn and others, 1998; Krimmel, 2001; Motyka and others, 2003). Equations (1) and (2) indicate that this must reflect seasonal variations in ice speed at the terminus, calving rate or a combination of the two. Here we document seasonal oscillations in terminus position at Hubbard Glacier, Alaska, (Fig. 1) using satellite images spanning the years 1992–2006. We present our data and explore the factors that may be influencing these variations as well as the stability of the terminus. In addition, we examine displacements of the medial moraine separating Hubbard and Valerie Glaciers at

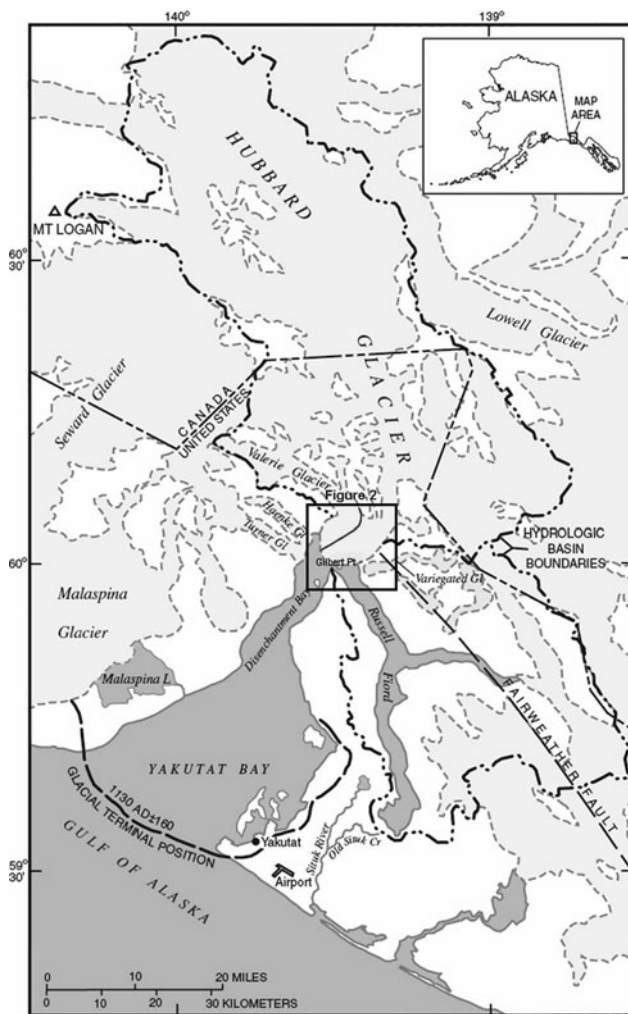


**Fig. 1.** Map of Hubbard Glacier showing maximum glacial extent in the early 1100s AD (modified from Trabant and others, 2003). The terminus is composed of ice from Hubbard and Valerie Glaciers, separated by a medial moraine.

the terminus (Fig. 1), and sea surface temperatures (SSTs) within the main area of Yakutat Bay and the adjacent Gulf of Alaska (GOA). It is thought that water temperatures affect calving of tidewater glaciers (e.g. Walters and others, 1988; Motyka and others, 2003). We investigate this by looking for possible relationships between changes in terminus position and SSTs.

## 2. HUBBARD GLACIER

Hubbard Glacier, with an area of 2450 km<sup>2</sup> (Arendt and others, 2002), is the largest non-polar tidewater glacier in the world. It descends >120 km from its origins, on the flanks of Mount Logan (5959 m) in Yukon, Canada, to sea level where it terminates in Disenchantment Bay and Russell Fiord near Yakutat, Alaska (Fig. 1). The height of the calving face ranges from 60 to 100 m a.s.l. and it has a curvilinear width of 11.5 km. On the western side of the terminus, the first 2 km is composed of ice originating from Valerie Glacier (Fig. 1).

Hubbard Glacier has historically revealed behavior that is asynchronous with regional glacier trends and seemingly independent of climate. Moraine deposits at the seaward entrance to Yakutat Bay (Fig. 1) indicate that the glacier filled

the entire bay as recently as AD 1100 (Plafker and Miller, 1958; Barclay and others, 2001). Water depths along this moraine average about 15 m and are nowhere deeper than 30 m. Barclay and others (2001) showed retreat was underway by AD 1380, and the records of A. Malaspina in 1792 and G. Vancouver in 1794 suggest that the head of the glacier was well into Disenchantment Bay by 1791 (Fig. 1). This implies a 410 year retreat during the Little Ice Age averaging 130 m a<sup>-1</sup>. This was a time when other glaciers throughout Alaska and northwest North America were advancing (Porter, 1989; Motyka and Begét, 1996; Wiles and others, 1999). Since first being mapped in 1895 by the International Boundary Commission, the glacier has advanced >2.5 km (Davidson, 1903; Trabant and others, 2003). This is in direct contrast to the regional trend: glaciers throughout Alaska and adjacent Canada have been retreating, some rapidly, during the past century (Arendt and others, 2002; Larsen and others, 2007).

Hubbard Glacier has a history of blocking the seaward entrance to Russell Fiord, which has a relatively large freshwater catchment area, thus creating a glacier-dammed lake (Fig. 1). Barclay and others (2001) showed that three major Holocene expansions of Hubbard Glacier have blocked Russell Fiord early in each advance. Twice in recent history the glacier has temporarily blocked the entrance to Russell Fiord; on both occasions the dam failed catastrophically (Motyka and Truffer, 2007). In April and May 1986 an emergent push moraine appeared at the terminus near the entrance to Russell Fiord, causing calving to stop. Mayo (1988, 1989) recorded a velocity of 36 m d<sup>-1</sup> in June 1986 on Valerie Glacier near its junction with Hubbard Glacier. Combined with observations of wrench faulting and mud and silty water being extruded from the terminus, this high velocity led Mayo to conclude that a surge of Valerie Glacier had occurred. Shallow waters near Gilbert Point facilitated the forward movement of a finger of ice which created an ice and push-moraine dam in May of 1986. The subsequent dam failure and lake outburst in October 1986 eroded the sediments near Gilbert Point to depths of 35 m or more (Trabant and others, 1991; Cowan and others, 1996). A 1999 US National Oceanic and Atmospheric Administration (NOAA) bathymetric survey showed that water depth averaged 25 m near Gilbert Point, suggesting a sediment infill in this area. In June 2002 an ice and push-moraine dam once again closed the entrance to Russell Fiord (Trabant and others, 2003; Motyka and Truffer, 2007). Heavy rain in August 2002 caused Russell Fiord to overtop the moraine dam, and rapid erosion resulted in dam failure accompanied by an outburst flood. The possibility of a sustained closure of Russell Fiord is of concern to Yakutat residents, as it may affect the Situk River, an important economic resource.

Hubbard Glacier is considered to be in the advance phase of the so-called tidewater glacier cycle (Post, 1975; Meier and Post, 1987; Post and Motyka, 1995; Trabant and others, 2003). The tidewater glacier cycle describes the cyclic behavior of slow advance and rapid retreat exhibited by calving glaciers grounded below sea level in fjords. Advancing calving glaciers, driven by a high accumulation-area ratio (AAR), advance into fjords by remobilizing subglacial sediments and by slowly pushing forward their terminal moraine shoals down-fjord (Hunter and Powell, 1998; Motyka and others, 2006). The typical advance rate for this process is a few meters to tens of meters per year. If,

for any reason, the terminus retreats from its terminal moraine shoal into deeper waters, an irreversible retreat can be initiated. This can occur when the glacier reaches mass-flux equilibrium at an AAR of approximately 0.7 (Post and Motyka, 1995; Trabant and others, 2003). Van der Veen (2002) suggests that thinning at the terminus of a tidewater glacier may also cause initiation of retreat. The rate at which a calving glacier retreats is typically on the order of 100–1000  $\text{m a}^{-1}$  (Meier and Post, 1987). Retreat then continues until the glacier terminus reaches a stable position, typically at a neck in the fjord or at the inland end of the fjord where the fjord bottom rises above sea level. Tidewater glacier retreat is often catastrophic, which rapidly increases the AAR, resulting in sufficient ice flux to once again advance the glacier. The remobilization of soft sediments, to create and maintain a terminal moraine, has been shown to excavate deep basins to well below sea level, which serves to accelerate calving during retreat (Motyka and others, 2006). A tidewater glacier can take many centuries to 1000 years to advance to the seaward end of its fjord (Meier and Post, 1987), but can retreat the same distance back up its fjord in only a few decades once stability from its moraine shoal is lost.

### 3. METHODS

#### 3.1. Image processing

Seasonal terminus positions of Hubbard Glacier were derived from satellite images for the period 1992–2006. The primary source for this dataset was synthetic aperture radar (SAR) images obtained from the Alaska Satellite Facility (ASF) at the University of Alaska Fairbanks. We have used images from the European Space Agency's ERS-1 and ERS-2 satellites and the Canadian Space Agency's RADARSAT-1 satellite. In a few cases, images were also obtained from NASA and the US Geological Survey's (USGS) Enhanced Thematic Mapper Plus (ETM+) instrument on board the Landsat 7 satellite. One image was also obtained from NASA's Advanced Spaceborne Thermal Emission and Reflection Radiometer (ASTER). We use radar imagery for its ability to record an image regardless of time of day and cloud cover, which is especially useful in coastal southeast Alaska where it is rarely clear. We have used standard beam SAR images which have 12.5 m pixel spacing. The resolution is similar for the Landsat images and the ASTER image which both have 15 m pixel spacing. An important characteristic of RADARSAT imaging which makes it suitable for this study is its 24 day repeat orbit. Since the area of interest (the region near the terminus of Hubbard Glacier) is small (270  $\text{km}^2$ ) compared to the image footprint (10 000  $\text{km}^2$ ), an exact repeat is not needed to capture the desired region. Our primary concern was to obtain images from roughly the same date each year, as opposed to obtaining exact repeat images.

Every image used in this study has been properly geocoded and co-registered in order to be compared within the same reference frame. Using ASF's Convert tool (<http://www.asf.alaska.edu/asf/?q=daac/softwaretools/mapready>), the images were geocoded to a Universal Transverse Mercator (UTM) projection using the World Geodetic System 1984 (WGS84) datum. Upon close inspection it was discovered that about 20 images were improperly co-registered and randomly shifted by 10–100 m. These images

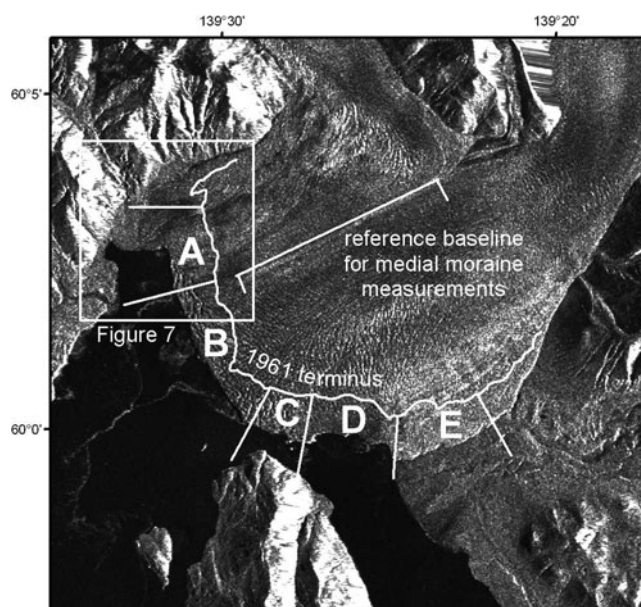


**Fig. 2.** The terminus of Hubbard Glacier separated into five sections based on contributing factors to terminus position. The location of Figure 7 is also shown, along with the reference baseline used to measure medial moraine displacement. © Canadian Space Agency 2003.

were co-registered by hand using Gilbert Point as a reference (Fig. 2). The Landsat images and the ASTER image were geocoded to the same datum and then co-registered by hand, using the same technique.

#### 3.2. Image analysis

We acquired a set of 59 separate terminus positions of Hubbard Glacier, spanning the period 1992–2006. The images were selected in order to establish a seasonal cycle. We limited our analysis to four images per year, which is sufficient to satisfy the Nyquist criteria for annual cycles. Ideally these positions would be taken in late January, early May, late July and mid-October. Since the 24 day repeat cycle of SAR satellites does not result in repeat images on the same date each year, it was not always feasible to obtain images at the same time each year. Therefore images were obtained as close to these dates as possible. Also, there are large data gaps, most importantly between December 2001 and September 2002. This gap is important because it spans the 2002 closure of Russell Fjord.

The terminus of Hubbard Glacier was divided into five sections, each of which can be distinguished by a different set of influencing factors (Fig. 2). Section A is made up of ice that flows from Valerie Glacier as defined by the medial moraine separating Valerie Glacier from the main branch of Hubbard Glacier. Here the terminus not only calves into Disenchantment Bay, but it also terminates on a mudflat. Section B is defined as ice flowing down from the main branch of Hubbard Glacier and terminating into the waters of Disenchantment Bay. Section C is defined by its proximity to Gilbert Point. To the east, section D calves into the waters of Russell Fjord. At the eastern end of the terminus, the land-terminating section E is advancing over glacier outwash deposits of nearby Variegated Glacier. Examining the behavior of each of these terminus sections separately is important for understanding variations of terminus position.

The location of the terminus was digitized in each of the satellite images. This was performed at approximately a 1:9000 scale. The 1961 location of the terminus was determined from USGS maps, which were made from aerial photographs (Fig. 2). This location provided a baseline for comparing the terminus positions acquired from the satellite images. The areas in each of the five polygons defined by the 1961 baseline, satellite terminus positions, and divisions between sections were measured on each image (Fig. 2). In order to compare one section with another, the changes in area were converted to average linear changes. Dividing the area of each polygon by its width resulted in a measurement of length which represents the total change in length since 1961 averaged over the entire section. Using the furthest east and west boundary lines, we similarly came up with a polygon and resulting change in length since 1961 averaged over the entire terminus. An additional terminus position was estimated for the Gilbert Point section (section C) for July 2002 using an aerial photograph taken by the US National Marine Fisheries Service (NMFS) during the closure of Russell Fiord. Using the photograph as reference, the terminus position was estimated and digitized in the same reference frame as the satellite images and processed in the same manner. It is important to note that we have used a constant width which we feel is representative for each section. Since the dividing lines are not parallel to each other, the width used does not reflect the non-constant width of each section. Therefore, the average linear change has relative but not absolute meaning, and should not be compared to similar data obtained by a different method.

### 3.3. Assessment of medial moraine displacement

We also used the satellite images to examine fluctuations of the moraine which separates Valerie Glacier from Hubbard Glacier. Due to snowfall covering the glacier, only the images taken in summer or fall showed this moraine clearly. We digitized the position of the moraine for all images in which it was distinguishable, which was typically only once per year. An arbitrary baseline was used as a reference (Fig. 2). Using the same technique used for the terminus change data, the moraine positions were combined with the reference baseline to determine areas with which to obtain width-averaged values of linear offset. In this manner, a time series of medial moraine movement was constructed. This dataset helps to establish the flow relationship between Valerie Glacier and the main branch of Hubbard Glacier.

### 3.4. Error assessment of image-derived data

The method we used for terminus digitization is somewhat subjective. Two sources of uncertainty arise from this process: (1) the error associated with the co-registration process, and (2) the uncertainty in terminus digitization. Because this region is highly glaciated and landscapes are constantly changing, the satellite images do not contain many features that can be confidently recognized from one image to another to use for co-registration. The region is also sparsely populated, and man-made features are not abundant. One feature that is easily distinguishable and visible on most of the images is the intersection of two runways at Yakutat Airport. We determined the coordinates of this location for 14 images and obtained a standard deviation of 18 m and 15 m for  $x$  and  $y$  respectively. The effect on the terminus of shifting an image along the  $x$  direction as opposed to the  $y$  direction depends on the terminus

orientation. To simplify, we have used the maximum possible error of 23 m.

The next source of error is the uncertainty in determining the terminus boundary. This uncertainty involves not only the pixel size of the image, but also the ability of an operator to effectively determine this boundary. We used two different methods to assess this error, both of which involve the repeatability of determining width-averaged change in length. For each of ten images, we repeated the terminus digitization process and, in doing so, obtained two distinct values of average linear change for each image. The standard deviation of the differences between these two values for the ten images is 9 m. The second method involved taking one image, repeating terminus digitization ten times, and processing these repeat digitizations to obtain an average linear change. The standard deviation of these average linear change values was 7 m. Since these two methods assess the same source of error, we have chosen the higher of these two values to represent this error. Whether or not an image is shifted does not affect the determination of the terminus boundary, so these two sources of error are independent. By error propagation, the overall uncertainty for an image-derived datum is  $\pm 25$  m.

### 3.5. Sea surface temperature

Some studies have indicated that ocean temperatures can affect the seasonal and perhaps the long-term stability of tidewater glacier termini (e.g. Walters and others, 1988; Motyka and others, 2003). Only sporadic temperature measurements are available within Disenchantment Bay (Motyka and Truffer, 2007). The best long-term temperature records are from satellite SSTs. We use these measurements as a proxy for water temperatures. We obtained spatially averaged, monthly SST records from NASA's Physical Oceanography Distributed Active Archive Center (PO.DAAC), which are derived from the five-channel Advanced Very High Resolution Radiometers (AVHRR) on board NOAA's polar-orbiting satellites. We have used the Pathfinder version 5.0 SST monthly data, which are a re-analysis of the AVHRR data stream developed by the University of Miami's Rosenstiel School of Marine and Atmospheric Science and the NOAA National Oceanographic Data Center. This re-analysis allows for an improved 4 km resolution and it has an accuracy of 0.5°C. Each monthly temperature record is the spatial average of temperatures derived within Yakutat Bay and the GOA. Re-analysis of the data stream results in a time lag between data acquisition and distribution. As a result, we were only able to obtain SST data up to 2004.

## 4. RESULTS

### 4.1. Terminus change

The results from the terminus position analyses are shown in Figure 3. The width-averaged change in terminus position since 1961 is given for each of the five sections (Fig. 3a–e), along with the change averaged over the entire terminus (Fig. 3f). The open circles represent the fall position for each year and help define the seasonal multi-year trend. The data gap in 2002 is a reflection of the lack of imagery at that time. The terminus position for Gilbert Point derived from the NMFS aerial photograph is represented by a dotted line in Figure 3c.

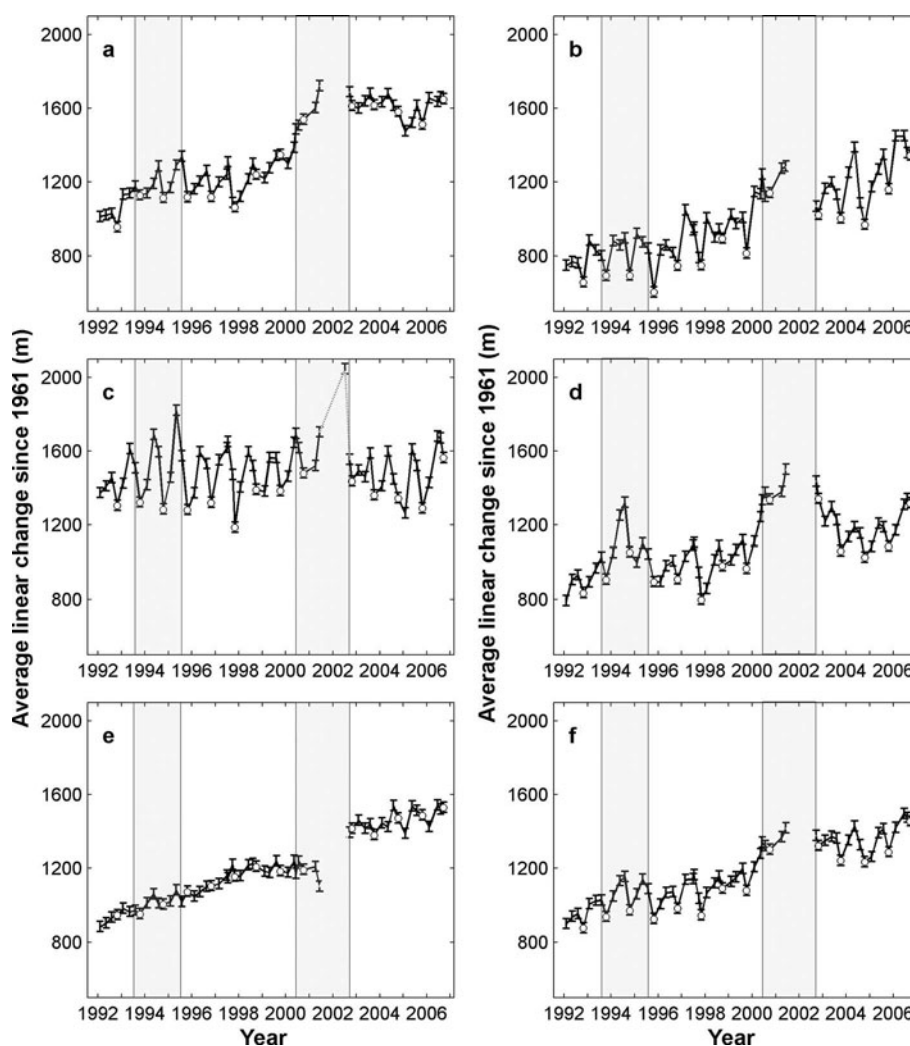


**Fig. 3.** Average linear change (with associated error) for (a–e) the five sections of Hubbard Glacier ((a) Valerie Glacier ice; (b) Disenchantment Bay; (c) Gilbert Point; (d) Russell Fiord; and (e) eastern land-based ice) and (f) the entire terminus. Circles represent fall position. Dotted line in (c) represents estimate of 2002 position from aerial photography. Shaded bars depict timing of medial moraine displacement events.

The section of the terminus consisting of ice from Valerie Glacier (Fig. 3a) shows a period of slow advance from 1992 to 2000 at an average rate of  $28 \text{ m a}^{-1}$ . This is followed by 2 years of accelerated advance which averages  $268 \text{ m a}^{-1}$ , and then an average advance rate of approximately  $0 \text{ m a}^{-1}$  from 2002 through 2006. Throughout all of these time periods, there exists a seasonal signal averaging around 100 m.

Section B, which is bounded by Disenchantment Bay, shows fairly regular behavior consisting of winter advance followed by summer retreat (Fig. 3b). Superimposed on an average advance rate of  $42 \text{ m a}^{-1}$  are seasonal fluctuations averaging 175 m. Retreats of up to 250 m occur over the time-span of only 2–3 months in late summer. Examination of images revealed that large embayments, 100–500 m in radius, form on average in about 50% of the summers.

The seasonal fluctuations seen near Gilbert Point are the most dramatic (Fig. 3c). These average 300 m and can be larger than 500 m in 1 year. Large seasonal changes in terminus position are superimposed over an average advance rate of only  $5 \text{ m a}^{-1}$ . The absence of any long-term advance rate, coupled with relatively large seasonal fluctuations, sets this region apart from the rest of the terminus.

The section of the terminus bounded by Russell Fiord exhibits the most erratic behavior of all the sections (Fig. 3d). While the 2006 position is further advanced than the 1992 position, this section fluctuated from advancing to retreating modes on timescales of several years. Large advances occurred in 1993–94 and 1999–2000 at rates of  $520 \text{ m a}^{-1}$ . These large-scale advances were soon followed by retreats of similar magnitude. Examination of Figure 2 shows that this section has a unique geometry, with a bay-like appearance. During these periods of accelerated advance and retreat, the change in terminus position occurs almost exclusively in the western end of this section, closest to Gilbert Point.

The land-based section of the terminus shows no signs of seasonal fluctuation (Fig. 3e) and has been advancing at a uniform rate of  $43 \text{ m a}^{-1}$ . The change in position for the entire terminus (Fig. 3f) over the time period of this study is remarkably uniform. An examination of the five individual sections of the terminus might lead one to predict that the trend for the entire terminus should be complicated. However, it appears that the somewhat erratic behavior in some of the individual sections cancels out when integrated across the terminus, resulting in an almost uniform advance of the entire terminal face, with a steady seasonal signal

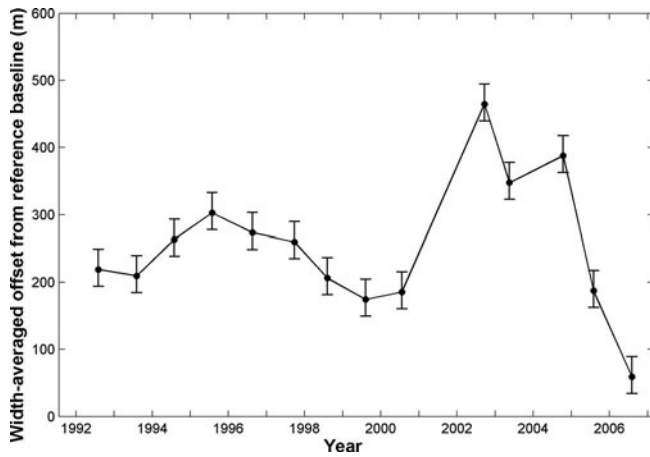


**Fig. 4.** Time series of medial moraine offset relative to an arbitrary reference baseline. Values of offset are averaged over the length of the baseline.

superimposed. The terminus advances throughout the winter and reaches its furthest extent by spring. It then undergoes retreat during the summer, and by fall the most retracted position is attained. During a typical year, the average position of the terminus fluctuates by 125 m. This seasonal cycle is consistent for the entire interval of this study, with the overall trend being slow advance. Throughout this period, the terminus has advanced approximately 620 m at an average rate of  $35 \text{ m a}^{-1}$ . Since 1961 the entire terminus has advanced an average length of 1495 m, which reflects a similar average advance rate of  $33 \text{ m a}^{-1}$ .

#### 4.2. Medial moraine displacement

Examination of the medial moraine separating Hubbard Glacier from Valerie Glacier (Fig. 2) revealed two distinct displacement events during the time period of this study (Fig. 4). From August 1993 to August 1995, the moraine was offset, on average, 100 m to the southeast. Over the next 4 years the moraine shifted back to the northwest, and by August 1999 it had returned to roughly the same configuration that it had occupied in 1992. A second displacement,

averaging 280 m, occurred between July 2000 and September 2002. This large offset to the southeast was followed by a similar but opposite offset to the northwest over the following 4 years.

#### 4.3. Sea surface temperature record

The spatially averaged, monthly mean SST record is shown in Figure 5. The seasonal variability in temperature ranges from  $10^\circ\text{C}$  to  $12^\circ\text{C}$ . Typically the coldest temperatures occur during December–March, with little variability during these months. The warmest temperatures are seen in July–September, but the variability in summer temperatures can be as high as  $4^\circ\text{C}$ .

### 5. DISCUSSION

#### 5.1. Interpretation of medial moraine movement

We interpret the displacement events seen in the medial moraine as representing an increase in the flow of ice of Valerie Glacier. Valerie Glacier has been shown to exhibit surge-like behavior in the past (Mayo, 1988, 1989). Visual inspection of imagery reveals that moraine patterns on Valerie Glacier during the 1993 and 2000 displacement events show a similarity to those seen in 1986. Landsat images acquired before and after the 1986 damming of Russell Fiord (<http://edc.usgs.gov/earthshots/slow/Hubbard/Hubbard>) reveal that a loop moraine was formed on a medial moraine separating two trunks of Valerie Glacier (Fig. 6). This also coincided with contortion of this moraine further up-glacier near the junction with Hubbard Glacier. During the time frame of the 1993 and 2000 displacement events, this moraine exhibited similar looping near the terminus and contortion further up-glacier. This may suggest that the surge-type behavior of Valerie Glacier may originate from one specific branch. We do not speculate here on the details of this. However, we do interpret the behavior seen in 1986 as being of the same type as that observed in 1993 and 2000. Our data suggest that Valerie Glacier may undergo these pulses on a somewhat regular basis, with a periodicity of several years rather than decades, as is the norm for surge-type glaciers (Raymond, 1987). These pulses also appear

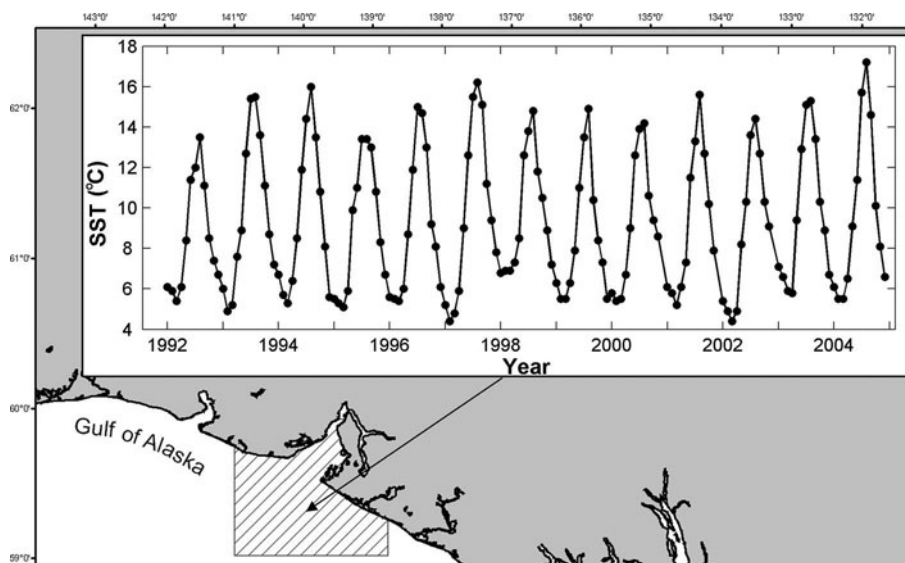


**Fig. 5.** Monthly mean SSTs spatially averaged over the shaded area within Yakutat Bay and extending into the Gulf of Alaska.



**Fig. 6.** USGS Landsat images acquired before and after the 1986 damming of Russell Fiord reveal contorted and looped medial moraine on Valerie Glacier. Similar moraine behavior was observed in 1993 and 2000.

weaker than a full-scale glacier surge (Meier and Post, 1969; Clarke, 1987; Harrison and Post, 2003).

Figure 3a shows that the timing of the second displacement event coincided with an advance of the terminus. This section began to advance at an accelerated rate in 2000, which continued until the 2002 data gap. After 2002, the rate of advance slowed considerably. Figure 7 shows the terminus positions for section A before 2000 compared to those after 2002. The position of the terminus fluctuated from year to year, but both the pre-2000 and post-2002 positions are tightly clustered. Between 2000 and 2002 the terminus advanced at an accelerated rate, but only onto land. In contrast, the seaward portion of section A showed little variation. The advance on land is consistent with the idea that a small 'surge' of Valerie Glacier occurred at this time. We suggest that the section of the terminus ending in water was not able to advance significantly because of deeper water seaward of the submerged moraine crest. An advance over this crest would bring the glacier closer to flotation, and calving would increase, forcing the terminus to calve back to a stable position. Where the ice terminates onto land, an increase in speed would advance the terminus at an accelerated rate. Figure 3a reveals that timing of the 1993 displacement event may also have coincided with a small change in terminus position, but temporal resolution of moraine positions does not allow for a definitive conclusion.

The sections of the terminus near Gilbert Point exhibited signs of having been affected by both medial moraine displacement events (Fig. 3c and d). During the winter of 1993/94, section C advanced 300 m. By October 1994, it had calved back to approximately the same position that it had held in the fall of both 1992 and 1993. Through the winter of 1994/95, this section of the terminus advanced >540 m to within 100 m of Gilbert Point. Once again, the ice had calved back to approximately the same fall position by October. These large-scale fluctuations in terminus position occurred simultaneously with the 1993 displacement event. Given the trend for 1992–95, one might have expected that Hubbard Glacier would have closed off Russell Fiord in 1996, but it did not. Rather, the terminus near Gilbert Point returned to earlier behavior for the years 1996–2000. The moraine displacement event in 2000 appears to have

affected this section of terminus in a similar fashion. Starting in the winter of 2001, section C advanced 570 m and blocked the entrance to Russell Fiord in June 2002 (Fig. 3c). This advance occurred simultaneously with the 2000–02 displacement event. Section D also experienced accelerated advance in 1994 as well as 2000, 2001 and 2002 (Fig. 3d). Given that the 1986 surge event and the 1993 and 2000 displacement events of Valerie Glacier all resulted in accelerated advance near Gilbert Point, it stands to reason that the flow relationship between Hubbard and Valerie Glaciers has a strong influence on terminus position in this region. This suggests that increased lateral ice flux into lower Hubbard Glacier caused by surges of Valerie Glacier may be a causal factor in the advances of terminus section C (Fig. 2) that block the entrance to Russell Fiord at Gilbert Point.

## 5.2. Ice speed and terminus position

Based on photogrammetric analysis, Trabant and others (2003) reported center-line ice velocities near the Hubbard

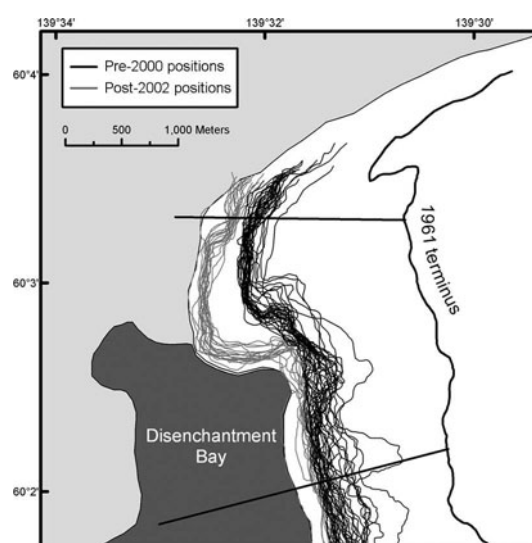


**Fig. 7.** Terminus positions for the Valerie Glacier section (section A) before and after the 2000 medial moraine displacement event. Accelerated advance onto land suggests a surge-type event.

Glacier terminus of  $11.5 \text{ m d}^{-1}$  in 2001. They also documented seasonal variations in surface ice speed of as much as  $2 \text{ m d}^{-1}$ . Center-line ice velocities near the terminus were  $9.1 \text{ m d}^{-1}$  from September 1988 through March 1989 (R. Krimmel, unpublished data). Krimmel also measured a center-line velocity near the terminus of  $13 \text{ m d}^{-1}$  from April through May of 1989. The general trend was that speed increased throughout the winter, with a maximum occurring in May and June. This speed maximum coincided with the time frame when the terminus typically advanced (Fig. 3). During late summer, surface speed decreased, reaching a minimum sometime between September and November. This minimum coincided with the time of typical seasonal terminus retreat (Fig. 3). If calving speed is held constant throughout the year, seasonal speed variations of  $2 \text{ m d}^{-1}$  could account for up to 360 m of seasonal terminus change according to Equation (1). The surface speed also varied spatially across the terminus. Typical observed speeds near the terminus were: section A,  $\sim 4 \text{ m d}^{-1}$ ; section B,  $\sim 13 \text{ m d}^{-1}$ ; sections C and D,  $\sim 6 \text{ m d}^{-1}$ ; and section E,  $< 1 \text{ m d}^{-1}$  (R. Krimmel, unpublished data).

While the seasonal variations in ice speed could, in principle, explain the seasonal fluctuations in terminus position, the spatial variations suggest that iceberg calving speed must also vary across the terminus. Observations of other tidewater glaciers have shown that calving varies seasonally. This strongly suggests that the observed changes in terminus position are functions of seasonal changes in both the forward component of the ice velocity and the calving velocity. It is apparent that variations in calving velocity and ice velocity contribute to the seasonality of the terminus position, but other factors must also be considered.

### 5.3. Water temperature and terminus position

Keeping in mind the difference in temporal resolution between the two datasets, there is an obvious correlation between seasonal fluctuations of terminus position and SST. In a typical year, water temperatures increase  $10\text{--}12^\circ\text{C}$  between April and August, and then decrease a similar amount between August and December (Fig. 5). In comparison, the terminus positions show a general trend of advance between October and May, followed by retreat from May to the following October (Fig. 3).

Because our record of terminus positions shows a strong seasonal signal, it could be correlated to any other dataset exhibiting a seasonal signal. However, consideration of the influence of sea-water temperature on terminus position comes from  $Q_c$  in Equation (2), which includes submarine melting. The model of submarine melting, and related calving, proposed by Motyka and others (2003) is a function of both the temperature of incoming saline water and subglacial freshwater discharge. Upwelling of fresh water along the submerged ice face drives convection of relatively warm saline ocean water. The resulting turbulent mixture melts glacier ice as it rises to the surface and forms an outflow plume of brackish water. High summer subglacial freshwater discharge and warm sea water result in greater submarine melting. The 15 m deep barrier moraine at the entrance to Yakutat Bay likely has a strong influence on the waters that enter Yakutat and Disenchantment Bays. This shallow moraine restricts inflow to the upper water column from the Gulf of Alaska. From April through August, surface water temperatures increase, supplying warm saline water to the bay and eventually the terminal face, increasing

submarine melting and iceberg calving. The summer increase in iceberg calving and submarine melting should increase the rate of retreat of the terminus (Equations (1) and (2)). Typically, we see such a retreat between May and October (Fig. 3). Evidence for 'warm' sea water in Disenchantment Bay near the ice terminus during late August was reported by Motyka and Truffer (2007), who found that late-August water temperatures at 50 m depth averaged  $9\text{--}10^\circ\text{C}$ . In contrast, April water temperatures at the same depth were  $3\text{--}5^\circ\text{C}$ . The decrease in water temperature from August to December is typically followed by a period of relative cold stability. Low temperatures throughout December–March rarely vary by more than  $1^\circ\text{C}$ ; this, combined with very low or absent freshwater discharge, results in little to no calving, according to the convection model. Without strong calving at the terminus, the influx of ice into the terminus dominates Equation (2), driving the position of the terminus forward. Accordingly, our observations (Fig. 3) show that the terminus advances between October and May each year.

The model of convection-driven melting at the submarine ice face (Motyka and others, 2003) is strengthened by our observation of embayments opening in the terminal front along Disenchantment Bay. We suggest these embayments are formed by localized increases in calving due to discharge streams emerging from beneath the terminus, which force convection and lead to submarine melting and undercutting of the face. The embayments only appeared along the section of the terminus bounded by Disenchantment Bay, primarily in the western half of section B (Fig. 2). The embayment locations did shift from year to year, indicating that the subglacial hydrological system changed with time. These openings were only observed in summer or fall and closed by winter, causing the terminal face to once again attain a relatively uniform geometry. Increased freshwater discharge at the terminus during the summers drove fjord sea-water convection, drawing warm saline waters to the calving front. We note that, during mid- to late summer, subglacial freshwater discharge was also at its peak from surface melt on the glacier. Further, this period coincided with the times when SSTs were at their seasonal highs (Fig. 5). Therefore, the increased convection occurred during times when the warmest saline water existed at the calving front. At LeConte Glacier, Motyka and others (2003) showed that submarine melting in late summer contributed about 57% of the estimated total ice loss at the terminus.

While large seasonal fluctuations are seen in both terminus position and SST, a correlation between annual changes in SST and terminus position is not apparent. One might expect that unusually warm summer water temperatures, such as those seen in 2004, would result in relatively high calving rates, and therefore a larger seasonal retreat compared to other years. Similarly, relatively warm winter water temperatures, such as those seen in 1997/98, might be expected to cause increased calving and result in a relatively small seasonal advance. These correlations at the terminus did not occur consistently. For example, the Disenchantment Bay section of the terminus (Fig. 3b) exhibited a large winter advance in 2001/02 corresponding to relatively low water temperatures (Fig. 5). However, the winter of 1996/97 showed a similar water temperature record but the terminus experienced average advance during this time period. These inconsistencies can be found throughout the SST record. This lack of correlation may, in part, be due to the relatively small

changes in temperature seen from year to year (1–2°C) compared to the seasonal variations (10–12°C). Also, note there is a 0.5°C uncertainty in the temperature data. Changes in the rate of ice delivery to the terminus caused by flow variations also play a role (as indicated by Equation (1)). Work by Motyka and others (2003) suggests that, while water temperature undoubtedly is significant for submarine melting of the terminus, the role of convection, driven by freshwater plumes of subglacial water, is the dominant process forcing increases in calving sufficient to cause substantial summer retreat and embayment formation.

#### 5.4. Water depth and terminus position

Water depth at the terminus has been shown to be a key factor in calving of tidewater glaciers (Post, 1975; Brown and others, 1982; Meier and Post, 1987; Van der Veen, 1996; Motyka and others, 2003). According to Brown and others (1982), the annual average calving speed is linearly dependent on the average water depth at the terminus. The model proposed by Van der Veen (2002) uses a height-above-buoyancy criterion for terminus position. Both models require knowledge of water depth; at an advancing glacier, such as Hubbard, the bed geometry is highly variable with time due to the ever-changing moraine crest. While the 60–100 m ice cliff places the terminus well above flotation, Van der Veen's model may be applicable as the terminus advances past the anchoring moraine into deeper waters. In such a situation, this model would require the glacier to calve back to a position where the water depth satisfies the height-above-buoyancy criterion. This provides a mechanism to explain how changes in ice speed are accommodated by similar changes in calving speed. However, application of this model would require an accurate knowledge of water depth at the terminus as a function of time. Unfortunately, repeat measurements of water depth along the calving front of a glacier like Hubbard would be both dangerous and expensive.

Tidal currents, water temperature and water depth have been shown to be important factors in controlling the position of terminus section C at Gilbert Point. Motyka and Truffer (2007) have shown how water depth in the gap near Gilbert Point has changed with time. The steady accumulation of glaciomarine sediments in Gilbert gap resulted in steadily decreased water depth in the gap. This trend was reversed by both the 1986 and 2002 outburst floods, which rapidly eroded the sediments, increasing water depth. Motyka and Truffer (2007) suggest that sediments must once again accumulate to a sufficiently shallow depth within the gap before another closure of Russell Fiord can occur.

We propose that decreasing water depth augmented by increased flow velocity at the Gilbert Point section of the calving front, caused by pulses (or actual surges) of Valerie Glacier (see Equation (1)), are important causal factors contributing to periodic closure of Russell Fiord. This was the case in 1986, when closure was accompanied by shallow water in Gilbert Point gap and a surge of Valerie Glacier. The relatively weak 1993 Valerie Glacier pulse similarly caused the terminus near Gilbert Point to advance an abnormally large distance for two years in a row (Fig. 3). However, each summer the terminus calved back to approximately its previous position. During this period, however, the water in Gilbert Point gap was still relatively deep as a result of the 1986 outburst flood. Not enough time had passed for the accumulation of glaciomarine sediments

to yield sufficiently shallow water. A combination of insufficiently shallow water, warm sea water and strong tidal currents forced the Gilbert Point section of the terminus to calve back to its former stable position.

By 2002, after a further 8 years of sediment accumulation, the water in Gilbert Point gap was sufficiently shallow to inhibit calving and associated submarine melting fueled by tidal currents. At this time, a pulse, or perhaps weak surge, from Valerie Glacier appears to have occurred. This pulse may have provided a 'sideways push' to the glacier, causing an increase in ice velocity in the corner between Disenchantment Bay and Russell Fiord, forcing an advance towards Gilbert Point. We believe that this advance, combined with inhibited calving due to shallow water, is what caused closure of the Gilbert Point gap and thus blockage of the entrance to Russell Fiord.

Surging of a much smaller tributary on the upper reaches of Hubbard Glacier was witnessed in 2000, while flying over the area, by K. Echelmeyer (personal communication, 2007). It seems unlikely that this would have had a significant effect on ice velocities at the distant down-glacier terminus, but it is important to note that surging of large up-glacier tributaries could, in principle, cause increased flow velocities at the Hubbard terminus analogous to those caused by pulses of Valerie Glacier. Since most of the tributaries of Hubbard Glacier are in the accumulation area, however, detection of tributary surges using SAR imagery might be problematic.

#### 5.5. Implications for terminus stability

The initiation of retreat of a large advancing tidewater glacier is among the large unknowns of the 'tidewater glacier problem'. How far, for instance, can the terminus retreat from its terminal moraine shoal during mid- to late summer before it becomes incapable of readvancing to its former position of stability, and retreat becomes catastrophic? We observed seasonal retreats of the terminus of Hubbard Glacier as large as 500 m, yet a full-scale retreat was not initiated. In fact, after each large retreat the terminus readvanced to a position even further down-fjord the following spring.

Columbia Glacier has exhibited similar seasonal variations in terminus position (Krimmel, 2001). From 1977 to 1982, it experienced average retreats of ~300 m between early summer and late fall. However, the terminus only advanced about half of that distance during the subsequent winters. Beginning in 1982, Columbia Glacier began its catastrophic retreat. During summers, retreats have averaged ~1000 m; sometimes up to 1500 m. Winter advances have been less than half these distances.

One difference that sheds light on why Hubbard Glacier is advancing, while Columbia Glacier is retreating catastrophically, can be found in the rates of elevation change of both lower glaciers. Extremely negative mass balances were measured and mapped by Meier and others (1985) on lower Columbia Glacier. They showed that the lower glacier was losing mass from ablation and flow to the calving front much more rapidly than it could be replaced by flow from up-glacier. Repeat aerial photogrammetric mapping showed that the surface of the lower glacier was lowering rapidly. This behavior is not characteristic of Hubbard Glacier, which has a large and relatively high-altitude accumulation area, a relatively small ablation area and an AAR more than 0.9. This high AAR should drive strong advance but in fact it

is almost completely balanced by iceberg calving, resulting in the slow advance we see today. In addition, Hubbard Glacier, unlike Columbia Glacier, is not experiencing rapid surface lowering in its lower reaches. Rather, Trabant and others (2003) observed increasing surface elevations near the terminus of Hubbard Glacier.

Pfeffer (2007) analyzed how different ratios of ice density times ice thickness ( $\rho_i h$ ) to water density times water depth ( $\rho_w d$ ) affected a standard sliding law (e.g. Budd and others, 1979). He found that as long as  $(\rho_i h)/(\rho_w d)$  remains above some threshold level ( $> \sim 1.3$ ), the terminus is relatively impervious to small perturbations in ice thickness and remains stable. This is because the driving stress is the primary control on sliding velocity (and therefore ice flux) when  $(\rho_i h)/(\rho_w d)$  is above the threshold value. For glaciers closer to flotation ( $(\rho_i h)/(\rho_w d) < \sim 1.3$ ), the effects of the effective pressure at the bed predominate, and the glacier becomes unstable because basal motion increases dramatically as the terminus approaches flotation. This increase in ice velocity also seems to lead to increased rates of calving and therefore thinning, thus initiating rapid tidewater retreat. Pfeffer's (2007) analysis for the available Hubbard data suggests that the glacier is above this threshold value, so small amounts of thinning will not lead to glacier acceleration. Thickness variations at the terminus might be caused by changes in flow originating up-glacier. Over long time periods, thickness changes on the lower glacier can also be forced by sustained negative (or positive) mass balance. This raises the question whether climate warming could reverse the thickening trend observed by Trabant and others (2003) near the terminus of Hubbard Glacier. Pfeffer's (2007) analysis would suggest that if the ice surface slope dropped below a critical value of the (reverse) bed slope, the terminus would no longer be stable against a small retreat.

## 6. CONCLUSIONS

Our observations indicate that a combination of factors influences seasonal changes in terminus position. These include (1) changes in ice speed and calving rate, (2) the position of the moraine shoal, which stabilizes the terminus in an overall sense, and (3) seasonal increases in sea-water temperature and subglacial freshwater discharge, which drives convection at the calving front.

Continued accumulation of sediments in the gap is increasing the probability of another closure of Russell Fiord because of the associated reduction of calving rate. If a pulse of Valerie Glacier also occurs, this would likely accelerate the advance of the Hubbard terminus at Gilbert Point, causing Russell Fiord to be blocked once again.

We foresee two possible scenarios for future closures of Russell Fiord. In the first scenario, sufficient sediment accumulates in Gilbert Point gap to enable the terminus to advance and close the gap. In this case, the advance may or may not be facilitated by a pulse or surge of Valerie Glacier (or some other up-glacier tributary). This scenario may be followed by destruction of the dam, as before, due to erosion by an overtopping stream, leading rapidly to an outburst of the impounded Russell Lake.

Although a combination of fast tidal currents, warm saline water and decreasing water depth have resulted in little or no advance of the terminus into Gilbert Point gap during recent years, the steady advance of the rest of the terminus must eventually force advance at Gilbert Point as

well. In this second scenario, the terminus at Gilbert Point will be forced to 'catch up' to the rest of the terminus, because of increasing ice thickness and surface slope at Gilbert Point. This second scenario seems most likely to result in a long-term blockage of the entrance to Russell Fiord, accompanied by continuing advance of Hubbard Glacier into Disenchantment Bay and formation of a relatively long-lived Russell Lake. The hydraulic head resulting from the elevated surface elevation of a dammed Russell Lake may result in multiple additional dam formations, each followed by an outburst flood, perhaps with slowly increasing dam stability (Motyka and Truffer, 2007).

## 7. NOTE ON RECENT EVENTS

We wish to report the appearance of a new moraine near Gilbert Point at the time of submission of this paper (20 September 2007). Analyzing aerial photos obtained from B. Molnia (USGS, retired), sediments for the moraine appear to have been derived from a large subglacial stream exiting the terminus during early August 2007. The location of this subglacial stream, so far to the east and close to Gilbert Point, contrasts sharply with our SAR observations over the last two decades, in which the principal subglacial discharge was invariably located near or to the west of the center of the Disenchantment Bay terminus (Fig. 2). Subsequent air photos obtained from A. Arendt (NASA Goddard Space Flight Center) and G. Kalli (US Army Corps of Engineers) show that a subaerial apron of sediment, about 100 m in diameter, had formed in front of this part of the terminus, protecting it from calving. Although seasonal retreat is continuing elsewhere along the terminus, the deposition of large amounts of sediment in the vicinity of Gilbert Point close to a known shallow reef increases the probability of a closure during the 2008 spring advance and perhaps even earlier.

## ACKNOWLEDGEMENTS

We thank the NASA Solid Earth and Natural Hazards Program for supporting this work with grant NAG5-13760 (NRA-01-OES-05), the NASA Cryospheric Sciences Program for providing joint funding of this grant, and the Interdisciplinary Science in the NASA Earth Science Enterprise for providing support for this work with grant NNG04GH64G (NRA-03-OES-03). We thank R. Gens and A. Prakash for assistance with satellite image processing, A. Arendt and S. Zirnheld for assistance with analysis methods, and K. Echelmeyer, W. Harrison and C. Larsen for discussions that improved the manuscript. The paper was also greatly improved by comments from T. Jóhannesson and an anonymous reviewer.

## REFERENCES

- Arendt, A.A., K.A. Echelmeyer, W.D. Harrison, C.S. Lingle and V.B. Valentine. 2002. Rapid wastage of Alaska glaciers and their contribution to rising sea level. *Science*, **297**(5580), 382–386.
- Barclay, D.J., P.E. Calkin and G.C. Wiles. 2001. Holocene history of Hubbard Glacier in Yakutat Bay and Russell Fiord, southern Alaska. *Geol. Soc. Am. Bull.*, **113**(3), 388–402.
- Benn, D.I., C.W. Warren and R.H. Mottram. 2007. Calving processes and the dynamics of calving glaciers. *Earth-Sci. Rev.*, **82**(3–4), 143–179.

- Brown, C.S., M.F. Meier and A. Post. 1982. Calving speed of Alaska tidewater glaciers, with application to Columbia Glacier. *USGS Prof. Pap.* 1258-C.
- Budd, W.F., P.L. Keage and N.A. Blundy. 1979. Empirical studies of ice sliding. *J. Glaciol.*, **23**(89), 157–170.
- Clarke, G.K.C. 1987. Fast glacier flow: ice streams, surging and tidewater glaciers. *J. Geophys. Res.*, **92**(B9), 8835–8841.
- Cowan, E.A., P.R. Carlson and R.D. Powell. 1996. The marine record of the Russell Fiord outburst flood, Alaska, U.S.A. *Ann. Glaciol.*, **22**, 194–199.
- Davidson, G. 1903. *The Alaska boundary*. San Francisco, Alaska Packers Association.
- Harrison, W.D. and A.S. Post. 2003. How much do we really know about glacier surging? *Ann. Glaciol.*, **36**, 1–6.
- Hunter, L.E. and R.D. Powell. 1998. Ice foot development at temperate tidewater margins in Alaska. *Geophys. Res. Lett.*, **25**(11), 1923–1926.
- Jacobs, S.S., H.H. Hellmer, C.S.M. Doake, A. Jenkins and R.M. Frolich. 1992. Melting of ice shelves and the mass balance of Antarctica. *J. Glaciol.*, **38**(130), 375–387.
- Krimmel, R.M. 2001. Photogrammetric data set, 1957–2000, and bathymetric measurements for Columbia Glacier, Alaska. *USGS Water-Resour. Invest. Rep.* 01-4089.
- Larsen, C.F., R.J. Motyka, A.A. Arendt, K.A. Echelmeyer and P.E. Geissler. 2007. Glacier changes in southeast Alaska and northwest British Columbia and contribution to sea level rise. *J. Geophys. Res.*, **112**(F1), F01007. (10.1029/2006JF000586.)
- Mayo, L.R. 1988. Advance of Hubbard Glacier and closure of Russell Fiord, Alaska: environmental effects and hazards in the Yakutat area. *USGS Circ.* 1016, 4–16.
- Mayo, L.R. 1989. Advance of Hubbard Glacier and 1986 outburst of Russell Fiord, Alaska, U.S.A. *Ann. Glaciol.*, **13**, 189–194.
- Meier, M.F. and A. Post. 1969. What are glacier surges? *Can. J. Earth Sci.*, **6**(4), 807–817.
- Meier, M.F. and A. Post. 1987. Fast tidewater glaciers. *J. Geophys. Res.*, **92**(B9), 9051–9058.
- Meier, M.F., L.A. Rasmussen and D.S. Miller. 1985. Columbia Glacier in 1984: disintegration underway. *USGS Open File Rep.* 85-81.
- Motyka, R.J. and J.E. Begét. 1996. Taku Glacier, southeast Alaska, U.S.A.: Late Holocene history of a tidewater glacier. *Arct. Alp. Res.*, **28**(1), 42–51.
- Motyka, R.J. and M. Truffer. 2007. Hubbard Glacier, Alaska: 2002 closure of Russell Fjord and implications for future dams. *J. Geophys. Res.*, **112**(F2), F02004. (10.1029/2006JF000475.)
- Motyka, R.J., L. Hunter, K.A. Echelmeyer and C. Connor. 2003. Submarine melting at the terminus of a temperate tidewater glacier, LeConte Glacier, Alaska, U.S.A. *Ann. Glaciol.*, **36**, 57–65.
- Motyka, R.J., M. Truffer, E.M. Kruiger and A.K. Bucki. 2006. Rapid erosion of soft sediments by tidewater glacier advance: Taku Glacier, Alaska, USA. *Geophys. Res. Lett.*, **33**(24), L24504. (10.1029/2006GL028467.)
- O'Neel, S., K.A. Echelmeyer and R.J. Motyka. 2001. Short-term flow dynamics of a retreating tidewater glacier: LeConte Glacier, Alaska, U.S.A. *J. Glaciol.*, **47**(159), 567–578.
- O'Neel, S., K.A. Echelmeyer and R.J. Motyka. 2003. Short-term variations in calving of a tidewater glacier: LeConte Glacier, Alaska, U.S.A. *J. Glaciol.*, **49**(167), 587–598.
- Pelto, M.S. and C.R. Warren. 1991. Relationship between tidewater glacier calving velocity and water depth at the calving front. *Ann. Glaciol.*, **15**, 115–118.
- Pfeffer, W.T. 2007. A simple mechanism for irreversible tidewater glacier retreat. *J. Geophys. Res.*, **112**(F3), F03S25. (10.1029/2006JF000590.)
- Plafker, G. and D.J. Miller. 1958. Glacial features and surficial deposits of Malaspina District, Alaska. (Scale 1:125,000.) *USGS Misc. Geol. Invest.* 1–271.
- Porter, S.C. 1989. Late Holocene fluctuations of the fiord glacier system in Icy Bay, Alaska, USA. *Arct. Alp. Res.*, **21**(4), 364–379.
- Post, A. 1975. Preliminary hydrography and historic terminal changes of Columbia Glacier, Alaska. (Scale 1:10,000.) *USGS Hydrol. Invest. Atlas* HA-559.
- Post, A. and R.J. Motyka. 1995. Taku and LeConte Glaciers, Alaska: calving-speed control of Late-Holocene asynchronous advances and retreats. *Phys. Geogr.*, **16**(1), 59–82.
- Raymond, C.F. 1987. How do glaciers surge? A review. *J. Geophys. Res.*, **92**(B9), 9121–9134.
- Reeh, N. 1994. Calving from Greenland glaciers: observations, balance estimates of calving rates, calving laws. In Reeh, N., ed. *Report of a Workshop on 'The Calving Rate of the West Greenland Glaciers in Response to Climate Change', 13–15 September 1993, Copenhagen, Denmark*. Copenhagen, Danish Polar Center, 85–102.
- Rignot, E. and P. Kanagaratnam. 2006. Changes in the velocity structure of the Greenland Ice Sheet. *Science*, **311**(5673), 986–990.
- Sikonia, W.G. 1982. Finite-element glacier dynamics model applied to Columbia Glacier, Alaska. *USGS Prof. Pap.* 1258-B.
- Sohn, H.G., K.C. Jezek and C.J. van der Veen. 1998. Jakobshavn Glacier, West Greenland: thirty years of spaceborne observations. *Geophys. Res. Lett.*, **25**(14), 2699–2702.
- Trabant, D.C., R.M. Krimmel, and A. Post. 1991. A preliminary forecast of the advance of Hubbard Glacier and its influence on Russell Fiord, Alaska. *USGS Water-Resour. Invest. Rep.* 90-4172.
- Trabant, D.C., R.M. Krimmel, K.A. Echelmeyer, S.L. Zirnheld and D.H. Elsberg. 2003. The slow advance of a calving glacier: Hubbard Glacier, Alaska, U.S.A. *Ann. Glaciol.*, **36**, 45–50.
- Van der Veen, C.J. 1996. Tidewater calving. *J. Glaciol.*, **42**(141), 375–385.
- Van der Veen, C.J. 1999. *Fundamentals of glacier dynamics*. Rotterdam, A.A. Balkema.
- Van der Veen, C.J. 2002. Calving glaciers. *Progr. Phys. Geogr.*, **26**(1), 96–122.
- Walters, R.A., E.G. Josberger and C.L. Driedger. 1988. Columbia Bay, Alaska: an 'upside down' estuary. *Estuar. Coast. Shelf Sci.*, **26**(6), 607–617.
- Wiles, G.C., D.J. Barclay and P.E. Calkin. 1999. Tree-ring-dated Little Ice Age histories of maritime glaciers from western Prince William Sound, Alaska. *Holocene*, **9**(2), 163–173.